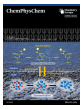

Speeding up Viedma Deracemization through Water-catalyzed and Reactant Self-catalyzed Racemization

Carola Tortora,[a] Christina Mai,[a] Francesca Cascella,[b, c] Michael Mauksch,*[d] Andreas Seidel-Morgenstern,[b, c] Heike Lorenz,[b] and Svetlana B. Tsogoeva*[a]

Viedma deracemization is based on solution phase racemization, dissolution of racemic or scalemic conglomerates and crystal growth through autocatalytic cluster formation. With rate limiting racemization, its acceleration by appropriate catalysts may result in speeding up deracemization. A conglomerate-forming chiral compound may principally racemize directly, or via reverse of its formation reaction. For a hydrazine derivative, we investigated available racemization pathways in presence of pyrrolidine or thiourea amine as base catalysts: via Mannich or aza-Michael reaction steps and their reverse, or by enolization. Racemization by enolization was computationally found to dominate, both under water-free conditions and in presence of water, involving a multitude of different pathways. Faster racemization in presence of water resulted indeed in more rapid deracemization, when the base was pyrrolidine. Under water-free conditions, the role of water as enolization catalyst is assumed by chiral hydrazine itself – in autocatalytic racemization and in which both reactant and product are catalysts.

1. Introduction

Demand of enantiomerically pure compounds significantly rose lately.[1] Chiral compounds are widely used for several applications, in cosmetic and agrochemical industry, fine chemicals production, as well as pharmaceuticals.[2] It is estimated that, among drugs produced and sold in last decades,[3] percentage of those approved as single enantiomer grew rapidly from 40 to almost 70% between 1991 and 2010.[1a] Development of processes that generate single enantiomers of chiral drugs which have been previously developed, approved and marketed as racemic mixtures, is driven partly by due expiration of intellectual property rights, seeing that routes to enantiopure compounds are usually more expensive and time consuming.[2,4]

Moreover,[5] demand for enantiopure products is supposed to increase dramatically in near future, due to inherent chirality of the biological environment.[2,6] Enantiopure drugs may have better pharmacodynamic or pharmacokinetic properties, less side effects or allow for an improved therapeutic width. Therefore, several methods have been already discovered and developed to obtain chiral compounds as single enantiomers. Besides asymmetric synthesis,[7] chiral resolution is still nowadays largely used, especially for industrial applications.[8–12] These methods are usually easy, fast and cheap ways to obtain enantiopure compounds, but highest affordable yields are 50%. Hence, a way to convert continuously one enantiomer into the other is needed. Combination of chiral resolution techniques with racemization methods allows to obtain up to quantitative yields.

A rather recent such methodology to quantitatively deracemize enantiomeric pairs of conglomerate-forming chiral compounds is Viedma ripening. Viedma first reported in 2005 complete deracemization of racemic conglomerates of $NaClO_3$.[13a] In this particular case, racemization is unnecessary, since starting material is already achiral in solution. Process of deracemization is a combination of non-linear autocatalysis during crystal growth and recycling through dissolution of crystallites spawned off from mother crystals by grinding.[13,14] When an intrinsically chiral molecule crystallizing as conglomerate is involved, racemization – usually an unwanted process in organic chemistry – is necessary here to obtain a completely homochiral final state.[15]

In 2009, we reported deracemization of a nearly racemic Mannich product, when its slurry was vigorously ground in presence of an appropriate achiral catalyst, based on our earlier observation of gradually increasing ee value in that Mannich product during an asymmetric synthesis from achiral precursors.[16] As was pointed out by us, such a combination of stereoselective reactions, starting from achiral reactants, with

[a] C. Tortora, C. Mai, Prof. Dr. S. B. Tsogoeva
Organic Chemistry Chair I and
Interdisciplinary Center for Molecular Materials (ICMM)
Friedrich-Alexander University of Erlangen-Nürnberg
Nikolaus-Fiebiger-Strasse 10, 91058 Erlangen (Germany)
E-mail: svetlana.tsogoeva@fau.de
[b] F. Cascella, Prof. Dr. A. Seidel-Morgenstern, Prof. Dr. H. Lorenz
Max Planck Institute for Dynamics of Complex Technical Systems
Sandtorstraße 1, 39106 Magdeburg (Germany)
[c] F. Cascella, Prof. Dr. A. Seidel-Morgenstern
Otto von Guericke University Magdeburg
Universitätsplatz 2, 39106 Magdeburg (Germany)
[d] Dr. M. Mauksch
Computer Chemistry Center
Friedrich-Alexander University of Erlangen-Nürnberg
Nägelsbachstrasse 25a, 91052 Erlangen (Germany)
E-mail: michael.mauksch@fau.de

Supporting information for this article is available on the WWW under https://doi.org/10.1002/cphc.202000493

Viedma deracemization could therefore effectively allow absolute asymmetric synthesis.[16] We proposed that racemization occurs *via* catalytic forward and reverse steps of the CC bond forming reaction, rather than by direct racemization of the centrally chiral product. Afterwards, we found that raising temperatures dramatically accelerated deracemization, which indicated that racemization is rate limiting in the whole process,[17] in contrast to other reports,[14,15] in which racemization was not considered rate limiting. In analogy to asymmetric autocatalysis by chiral monomers in solution,[18] we also surmised that racemization could be autocatalyzed by the conglomerates' crystal surface, due to observation that racemization time in solution is much longer than deracemization took under grinding conditions.[17]

Motivated by these early observations, we reasoned that with rate limiting racemization,[17] it should be possible to speed up deracemization itself by faster racemization! To elucidate mechanistic details of racemization under original water free conditions, we carried out DFT computations, phase diagram studies of the chiral Mannich product, racemization and deracemization experiments in a joint experimental and theoretical approach to investigate the racemization mechanisms of **1** (Scheme 1) and how they could be accelerated. We demonstrate herein that faster racemization indeed results in faster deracemization, when pyrrolidine is the base catalyst and in presence of water. To explain racemization of Mannich product under water free conditions, we also conceptually develop herein an autocatalytic racemization model and in which both reactant and product catalyze their respective transformation in a process, which extends, hence, the concept of (asymmetric) catalysis.

2. Results and Discussion

Melt phase diagram of the chiral system was determined *via* Differential Scanning Calorimetry (DSC) studies supported by coupled thermogravimetry-DSC (TG-DSC), Hot Stage Microscopy (HTM) and X-Ray Powder Diffraction (XRPD) measurements. Therefore, (*R*)-**1**, *rac*-**1** (Scheme 1) and molecular disperse mixtures of both were subjected to a DSC heating run to obtain respective melting DSC curves. Solidus and liquidus temperatures were determined from corresponding melting peak onsets or dissolution peak maximum temperatures.[19]

Figure 1 shows the melt phase diagram of chiral compound **1** with *rac*-**1** on the left and (*R*)-**1** on the right side of the composition axis. That is, only half of the phase diagram is given, as mirror image symmetry is implied in chiral systems. The steady course of the liquidus line connecting higher melting pure enantiomer (*R*)-**1** with significantly lower melting *rac*-**1** provides evidence of conglomerate behavior. This is also confirmed by identical XRPD patterns (see SI 1). The melting temperatures are found to be 142.4 °C for (*R*)-**1** and 125.8 °C for *rac*-**1**, respectively which well corresponds with HSM studies (see SI 2 and SI 3). It should be noted that melting of (*R*)-**1** and *rac*-**1** is accompanied by partial decomposition expressed by a mass loss of ca. 2.3% and 0.8% until the respective melting peak maximum. At the final heating temperature of 170 °C, ca. 9.9% and 11.1% mass loss were recorded for (*R*)-**1** and *rac*-**1**, respectively.

In addition, as shown in the Tammann plot (Figure 2), no miscibility in solid state is present in the system, which means that enantiomers do not form mixed crystals (or solid solutions), which is a desirable property with respect to any crystallization-based enantiomer separation. Initially, we focused our efforts on optimizing the racemization conditions in solution, at room temperature (Scheme 1).

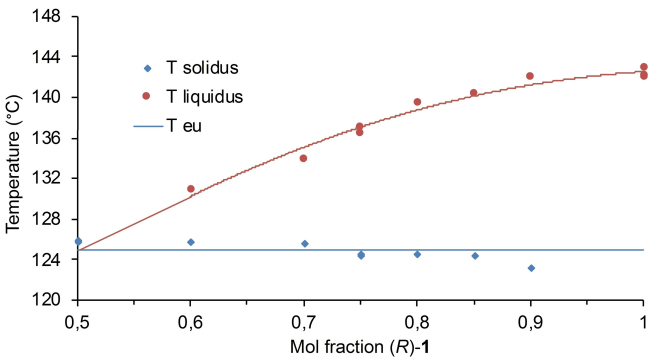

Figure 1. Melt phase diagram of *rac*-1 and (*R*)-1. Symbols denote measured solidus and liquidus temperatures (diamonds and circles, respectively). Lines represent solidus and liquidus lines, with the latter as guide to the eye and the solidus line derived from averaged solidus (eutectic) data.

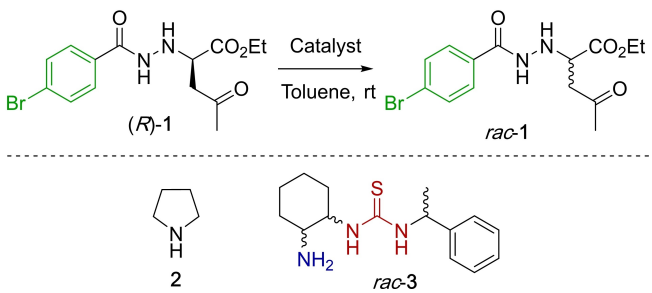

Scheme 1. Racemization experiments, carried out at room temperature on (*R*)-1, varying catalyst 2 and 3 loading.

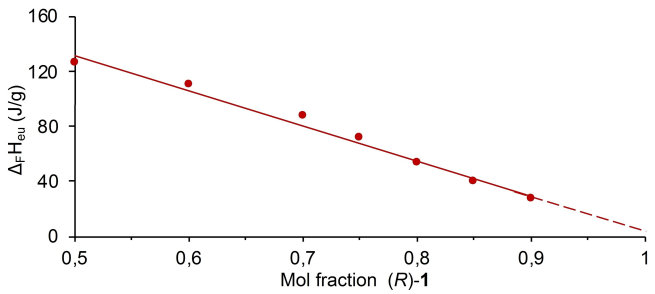

Figure 2. Tammann plot of heats of fusion of eutectic peak, $\Delta_F H_{eu}$, as a function of composition. Data points are linearly related and the extended straight line intersects with pure enantiomers' composition.[19]

We intended to use same catalytic systems as we have employed in our earlier works on deracemization.[16,17] The use of 0.5 eq *rac*-**3** and 0.25 eq pyrrolidine **2** proved to be a compromise between ensuring sufficiently fast racemization and low enough degree of decomposition, since using 1.0 eq of pyrrolidine caused decomposition of (*R*)-**1** after only 1.5 hours.

First, we evaluated effect of rac-3 on racemization of (R)-1, varying temperature and catalyst loading. Figure 3 shows measured ee values. Each reaction was sampled every 24 hours and directly analyzed without any further purification. Racemization occurred in all runs, albeit slowly at room temperature. Trend lines are not linear, indicating that racemization in toluene does not follow a first order kinetic. Under isothermal heating to 40 °C, racemization was considerably faster, and an ee value of 60.1 % was reached after 96 hours, when (R)-1 eventually decomposed.

Although racemization occurs in homogenous solution, none of the performed experiments exhibited a rate consistent with the speed of deracemization observed previously.[16,17] During Viedma deracemization processes, a slurry is ground at high stirring rates (up to 1300 rpm), i.e. the system is heterogenous with a crystal-solution interface present, and concentration of the target compound is much higher, thanks to supersaturation. Hence, we wondered if during Viedma deracemization, presence of a crystal-solution interface could result in higher racemization rates than those observed in more diluted - and homogenous - (gleiche wie oben) solutions.[20]

Hence, we tried to investigate effect of presence of a racemic crystal phase on racemization rate. In order to assess degree of racemization, we used a "mimic" of 1, namely rac-4 (Scheme 2),[21] bearing a nitro substituent instead of bromine in para position of the aromatic ring, seeing that enantiomers of 1 and 4 are well separable in chiral HPLC. Figure 4 shows somewhat faster racemization compared to results observed in homogeneous solution. After 48 hours, even starting from enantiopurity, 60 % ee was reached, while after the same time, without presence of a mimic solid phase, ee was still above 90 %, even though starting ee value was lower. Using (S)-4 as solid phase, with opposite absolute configuration at the stereocenter with respect to that in (R)-1, racemization was only a little bit faster than in homogenous solution - which could well be in range of experimental error (note that initial ee was higher, though). These findings lend some support to the idea that racemization may be positively influenced through a crystal-solution interface, whereas it does not mean that it occurs there exclusively, instead of deep in solution phase. Note also that it appears to be exactly the same (rather than oppositely) configured (quasi-)enantiomer, which has the largest effect in the heterogenous system.

Reversible Mannich type reaction proposed in our previous works,[16,17] was supposed to involve activation of acetone via enamine formation by nitrogen containing bases thiourea amine rac-3 or pyrrolidine and subsequent attack of this stronger nucleophile on aminoalkylating hydrazone substrate 5 (Figure 5). Conceivably, this reaction could also proceed in

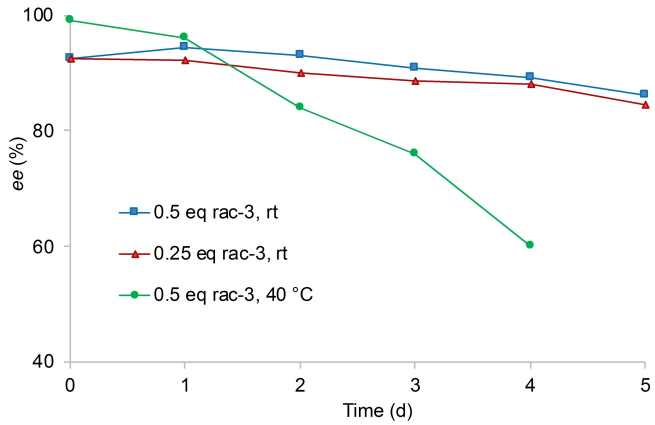

Figure 3. Racemization of (*R*)-1 using *rac*-3 as catalyst. *ee* values are measured from samples taken every 24 hours. Reaction conditions: (*R*)-1 in toluene (0.022 M) with 0.5 eq *rac*-3 at rt (□), 0.25 eq of *rac*-3 at rt (△), and at 40 °C using 0.5 eq *rac*-3 (○).

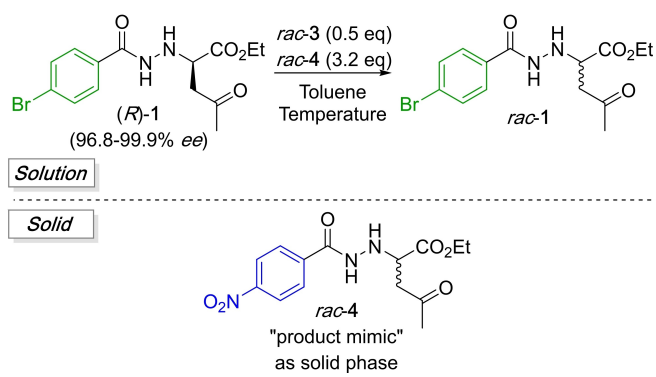

Scheme 2. Racemization in heterogeneous reaction mixture, using "mimic" *rac*-**4** as solid phase [3.2 eq with respect to (*R*)-**1**].

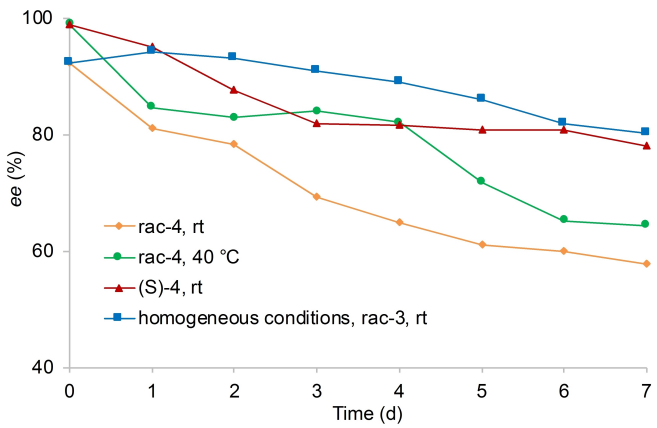

Figure 4. Racemization of (R)-1 using rac-3 as catalyst in presence of a racemic or homochiral (S) crystal phase of mimic 4. ee values of (R)-1 are measured from samples taken every 24 hours. Solution and crystalline phases of each sample were separated, and values reported correspond to solution phase analyses. Reaction conditions: (R)-1 in toluene (0.224 M) with rac-4 as racemic solid phase (3.2 eq with respect to 1) at room temperature (◇) and at 40 °C (○), and with (S)-4 as solid phase (3.2 eq with respect to 1) at room temperature (△). For comparison, we included a control experiment in homogenous solution [(R)–1 0.022 M in toluene] at room temperature (□).

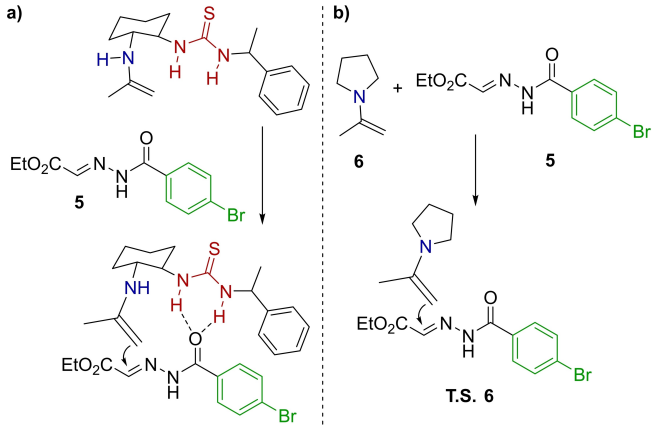

Figure 5. Mannich reaction steps, proposed to be involved in racemization mechanism of **1**, proceeding via enamine formation between *rac*-**3** a) or pyrrolidine b) and acetone, followed by attack on hydrazone.

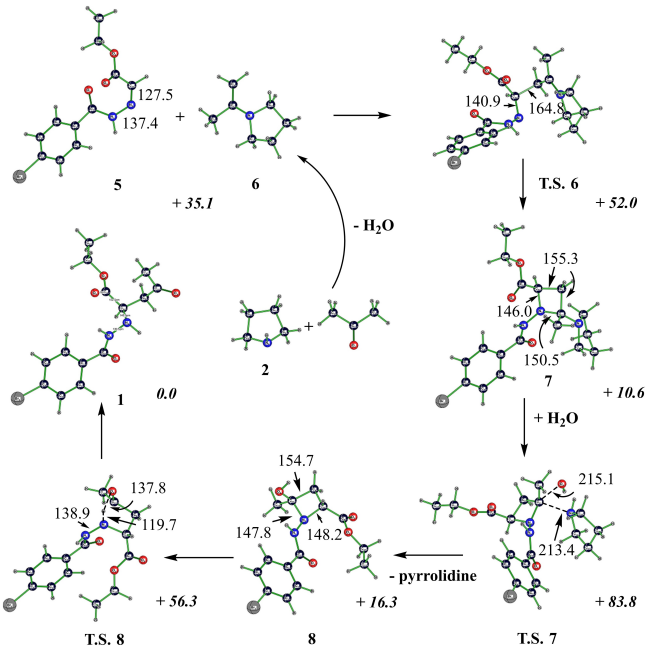

Figure 6. Computed M06-2X/6-31G* structures on reaction pathway for Mannich type reaction of hydrazone **5** with enamine **6** to give eventually chiral hydrazine **1** (see also Fig. 5b). Solvent effects have been included by polarizable continuum (PCM) model with electric permittivity of toluene. Selected bond lengths and distances are given in pm. Relative energies (in kcal mol^{-1}) are in italics.

reverse order to reproduce either enamine or acetone together with prochiral substrate, resulting in racemization via reverse reaction. Mass balance is only 25.8% yield of 1 (at 85.3% ee for a batch size of 86.6 mg), retrieved after deracemization, which indicates that many side reactions occur, reducing achievable yields of deracemized product after the grinding process. Hence, we wanted to understand in detail available racemization pathways.

DFT computations have been carried out only with more tractable pyrrolidine as organic base. At first, we studied computationally pyrrolidine assisted Mannich reaction, giving 1 from hydrazone 5 and enamine 6 (Figure 6). This reaction proceeds smoothly in forward direction with an activation barrier of 16.9 kcal mol^{-1} for CC bond forming and configuration determining step. Resulting intermediate is acetidine 7, which reacts further in proton transfer steps to recover pyrrolidine to give carbinolamine 8, which finally tautomerizes under ring opening to hydrazine derivative product 1. Barriers for proton transfer steps via T.S. 7 and T.S. 8 appear to be exceedingly high. However, exactly these transition state structures are supposed to profit most from stabilization by hydrogen bonding, when additional molecules with both hydrogen bond donor and acceptor capabilities were involved in the activated complex, as, e.g. pyrrolidine or water. As can be seen, reverse Mannich step from rather low energy acetidine towards reactant 5 and 6 level has a rather high barrier of 41.4 kcal mol^{-1}, and is hence unlikely to contribute much to the racemization process, at least deep in solution phase.

Alternatively, it is also conceivable that minority enol form of acetone is attacking hydrazone directly in an uncatalyzed reaction (see Figure SI 6 in the Supporting Information). However, acetone enol is even more endothermal (by 6.2 kcal mol^{-1}) than enamine 6. Consequently, activation barrier for CC bond forming step is, with respect to level of separated reactants, 15.9 kcal mol^{-1} higher in energy than process shown in Figure 6. As also an intermediate in acetone enol involving Mannich reaction, a hydroxyl ether, is even 22.9 kcal mol^{-1} higher in energy than carbinolamine 8, such an acetone enol mechanism can here almost safely be ruled out. A third, related, possibility (which we have not computed) and avoiding formation of hydroxyl ether, is non-covalently organocatalyzed attack of acetone enolate after deprotonation by pyrrolidine and eventual protonation of hydrazide anion after CC bond forming step.

Another conceivable possibility to racemize 1 via a combination of forward and reverse reaction steps could be the aza-Michael reaction (Scheme 3b). Indeed, in 2014 a Viedma deracemization experiment was reported, where base catalyzed racemization of a non-enolizable aza-Michael product in solution was proposed to proceed via a sequence of forward and reverse aza-Michael reaction steps,[22] similar to our earlier

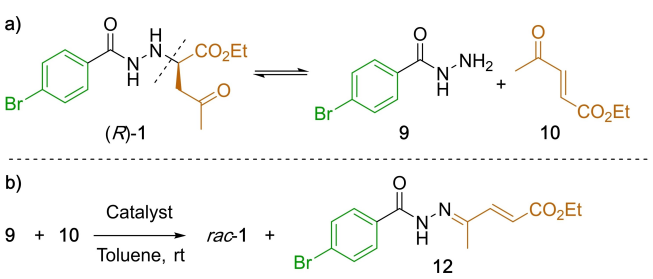

Scheme 3. a) Envisaged retro-synthetic pathway for racemization of (*R*)-**1** via forward and reverse aza-Michael reaction steps. b) Aza-Michael reaction between **9** and **10**, performed under same conditions as in racemization experiments (with 0.25 eq pyrrolidine or 0.5 eq thiourea amine in toluene at room temperature). For results, see text.

proposal for the Mannich reaction.[16] Even though the reactant was a primary amine, non-nucleophilic base 1,8-Diazabicyclo [5.4.0]undec-7-ene (DBU) was used as catalyst, as priorily it was reported that this base could assist in more sluggish aza-Michael reactions with secondary amines as substrates.[23] Therefore, we envisaged in a retro-synthetic manner, that 1 undergoes a reverse aza-Michael reaction to give Michael donor 9 and Michael acceptor 10 (Scheme 3, a).

DFT computations on mechanism of reverse aza-Michael reaction step starting from hydrazine derivative 1, is shown in Figure 7. Similar to situation for Mannich reaction (Figure 6), reverse step of CC bond forming 1,4-addition has a high activation barrier and proceeds via T.S. 10 to give separated Michael donor and acceptor, 9 and 10, respectively. Organic base is obviously not necessary to catalyze CC bond forming step due to sufficiently high nucleophilicity of the primary amine, and forward reaction requires an activation energy of only 10 kcal mol^{-1} with respect to reactant level. Hence, it appears that an aza-Michael/reverse aza-Michael sequence (albeit a little bit more favorable than the Mannich/reverse Mannich process above) is also not a promising candidate for rapid solution phase racemization, even though reverse Mannich or reverse aza-Michael reaction steps could, in principle, also contribute to racemization to some small extent.

Formation of main product 12 from aza-Michael precursors 9 and 10 showed the initial product being a carbinolamine 11 (Figure 7), giving condensation product 12 after removal of water, following a second tautomerization step. Barriers for proton transfer steps via T.S. 11 and T.S. 12 are rather high, without further catalytic assistance. Obviously and deplorably, pyrrolidine (and rac-3) are able to catalyze these steps, resulting in sufficiently low energy activation barriers for these proton transfers, which explains experimentally observed low yields in aza-Michael reaction, because unsaturated hydrazone 12 precipitates in the reaction medium and disrupts solution phase equilibria (Scheme 4). Indeed, carrying out aza-Michael reaction on precursors 9 and 10, applying conditions as used in racemization experiments in presence of pyrrolidine or rac-3 (Scheme 3b), rac-1 was obtained in both cases with only low yields of 26.4 % with 2 and of 8.3 % with rac-3, respectively.

Therefore, we had to look for a different and faster pathway to explain experimentally observed racemization and deracemization. Probably fastest way to invert configuration at a chiral carbon center is pyramidal inversion of a carbanion, resulting from deprotonation (with a barrier of about 2–3 kcal mol^{-1}).[24] On the other hand, deprotonation itself might take some time, depending on base and solvent.[25] Note the need for reversibility here, which precludes e.g. metal hydrides as deprotonating agents. Another possibility, albeit much slower than carbanion inversion, is base catalyzed enolization, which also involves initial deprotonation, giving first a mesomerism-stabilized enolate, unless enolization is concerted, yielding directly the enol. When an enolizable group is present, as in (R)-1 the ester carbonyl group in α-position with respect to chiral center, initial (catalytic) deprotonation at the chiral center results in immediate and smooth formation of an achiral enolate instead of a carbanion – tantamount to tautomerization, after enolate protonation.[26] The base should be strong enough to deprotonate a CH bond, which is often rate determining. Second step is protonation of carbonyl oxygen, giving the enol. Intriguingly, concerted enolization with a single pyrrolidine molecule involved, is disfavoured energetically by 6.2 kcal mol^{-1} with respect to a stepwise process. Preference for a step-wise process holds even when solvent is assumed being polar water, despite intermittent formation of an ion pair in step-wise enolization, probably because with protic base

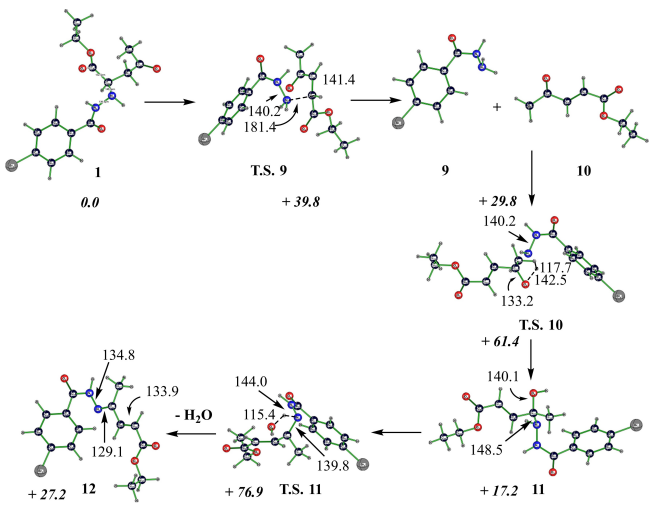

Figure 7. Computed M06-2X/6-31G* structures for reverse aza-Michael reaction of (*R*)-**1**, giving **9** and **10**, and their competing side reaction towards achiral condensation product **12** via carbinolamine intermediate **11** (see also Scheme 3a). Solvent effects have been included by polarizable continuum (PCM) model with electric permittivity of toluene. Selected bond lengths and distances are given in pm. Relative energies (in kcal mol^{-1}) are in italics.

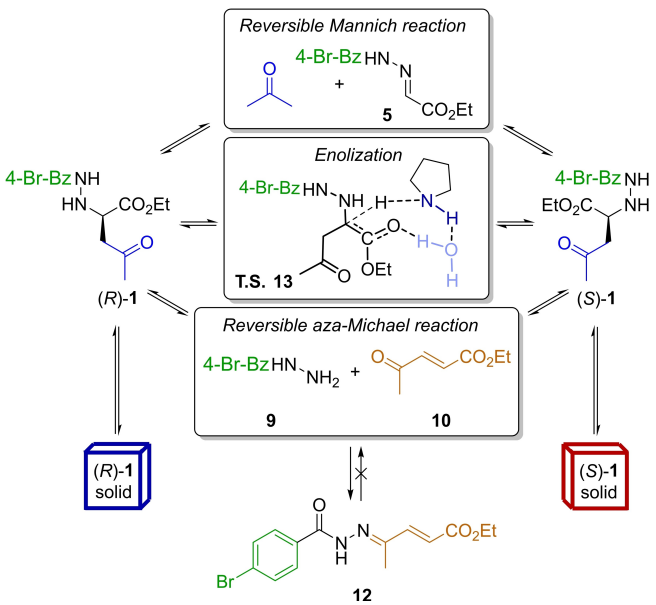

Scheme 4. Graphical representation of competing and conceivable base-catalyzed racemization pathways in deracemization of chiral hydrazine derivative **1** (cf. Figures 6–8). Reverse aza-Michael reaction favours formation of insoluble hydrazone **12**, thereby reducing achievable yield.

pyrrolidine, step-wise processes are always favoured and transition state structure comprises non-polar groups, that screen effectively the charge dipole in its center.

When deprotonation transition state involves two pyrrolidine molecules, it is 4.6 kcal mol^{-1} higher in energy than with one pyrrolidine and one water molecule. Water is obviously the better co-catalyst in enolization than pyrrolidine itself! Most strikingly, a single-pyrrolidine stepwise enolization mechanism is disfavoured by 23.0 kcal mol^{-1}1 with respect to the most preferred mechanism (Figure 8), involving one pyrrolidine and one water molecule in the transition state.

Hence we envisioned, that adding a "stoichiometric" amount of water (with a tentative 4:1 ratio with respect to base catalyst) should accelerate racemization of (R)-1, and, because of rate limiting nature of the racemization process, should allow to speed up deracemization, as well. Results of DFT computations for this racemization pathway are shown in Figure 8. Enolization begins with deprotonation by pyrrolidine at chiral carbon in α-position to carbonyl group of the ethyl ester moeity in 1 via T.S. 13 (Figure 8). This reaction step has a rather low energy barrier and proceeds readily to give a close ion pair of enolate and protonated pyrrolidine, 13, rather than a carbanion, because negative charge flows immediately to more electronegative oxygen atom of the carbonyl group instead of remaining localised at carbon. Activation barrier to form 13 from 1 is only seemingly negative (Figure 8), and is 20.3 kcal mol^{-1} with respect to a hydrogen bonded encounter complex, because reference level for reported relative energies is entry channel of separated reactants. In the second step, proceeding via T.S. 14, a proton is relayed from pyrrolidine to water and a second one from water back to enolate to give an achiral enol 14 as a rather unstable intermediate. Racemization results, when reprotonation at α-carbon takes place on the other (i.e. Si) face of the enol group, giving (S)-1.

Note that this reprotonation is principally possible by either conjugate acid of pyrrolidine or by a hydronium ion, generated by deprotonation of enol oxygen, again by either water or pyrrolidine. However, if any alternative pathway to that shown in Figure 8 would be energetically more favorable, microscopic reversibility demanded that the very same pathway must be followed preferably and in reverse order of steps, leading back to reactants. As concerted tautomerization is high in energy, enol formation occurs preferably by tautomerization steps as shown in Figure 8, and this holds, of course, also for the way back to either enantiomer of hydrazine derivative 1.

Please note, that enol 14 is conformationally chiral, despite absence of any chirality elements. Hence, racemization will only occur if free 14 is available in the reaction medium (i.e. after complex with base dissociated), because otherwise, tracing back the same pathway as shown in Figure 8 will result in rentention at chiral carbon of 1 through a "memory of chirality" effect.[27]

Seeking experimental confirmation of these insights, we performed experiments using pyrrolidine 2 as racemization catalyst with water as co-catalyst and compared the collected data with a similar control experiment without water (Table 1 and Figure 9). Additionally, presuming that a similar effect could actually occur also using thiourea amine rac-3 as catalyst, we performed similar comparative experiments with rac-3, too. The reaction conditions are summarized in Table 1.

These experiments confirmed that addition of 1 eq of H_2O has a positive (i.e. accelerating) effect on racemization rate.

Table 1. Reaction conditions for experiments of base catalyzed racemization of (*R*)-**1** in homogenous solution, with and without water.

Entry[a]	ee_0 [%][b]	Cat [eq][c]	H_2O [eq][c]	ee_{low} [%][d]
a	94.7	2 (0.25)	1.0	72,3
b	93.2	2 (0.25)	–	89,9
c	94.8	*rac*-3 (0.5)	1.0	72.2
d	94.8	*rac*-3 (0.5)	–	87,7

[a] Entries in table correspond to lines in Figure 9. [b] Measured from pure (*R*)-**1** by chiral HPLC. [c] With respect to (*R*)-**1**. [d] Indicates lowest (and final) *ee* measured, after an evaluation time of nine days.

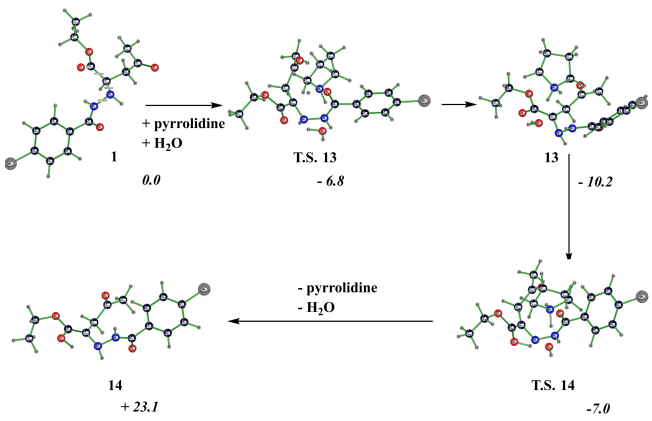

Figure 8. Computed M06-2X/6-31G* structures for step-wise enolization of (*R*)-**1**, catalyzed by a single pyrrolidine and a single water molecule (cf. Scheme 4, middle pathway). Solvent effects have been included by polarizable continuum (PCM) model with electric permittivity of toluene. Selected bond lengths are given in pm. Relative energies (in kcal mol^{-1}) are in italics and with respect to separated reactants.

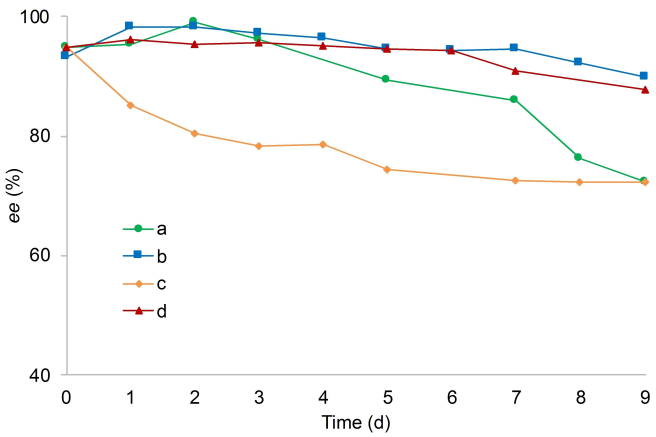

Figure 9. Corresponding *ee* values measured during racemization experiments in homogenous solution with and without H_2O as additive. Reaction conditions are reported in Table 1 (runs **a**–**d**).

Comparing lines a and b (Figure 9), corresponding to use of pyrrolidine either with and without water, respectively, ee-value measured after four days is already lower than in the corresponding experiment without additive, and at the end of the evaluation time it was possible to reach 72,3% ee, whereas without water, only a decrease to 89,9% ee was measured.

As expected, the effect hypothesized with pyrrolidine, was observed also using thiourea amine catalyst. As line c shows (Figure 9), effect of adding 1 eq of water is surprisingly strong (e.g. after nine days measured ee-value is already 72,2%, while without water, enantiomeric excess does not reach a lower value than 87.7% after the same time), seeing that thiourea possesses more than one basic site, and could, in principle, assist in enolization of **1** even without water.

While we have not sought here to optimize the ratio of water to base, we found that addition of, e.g., 10 eq of water does not result in any further acceleration of racemization, indicating that too large an excess of water may destroy the intricate hydrogen bonding network involved in the proposed enolization transition state (Figure 8), thereby blocking the fastest available racemization pathway. Water molecules may, for instance, more frequently replace much stronger base pyrrolidine in the transition state structure, resulting in less effective Cα deprotonation.

Next, we were curious whether an accelerated racemization will indeed also result in a more speedy deracemization process under Viedma deracemization conditions (Scheme 5).

We first evaluated deracemization starting from fully symmetric initial conditions, i.e. a racemic slurry of 1 in presence of rac-3, with and without water as additive (Figure 10). Glass beads were added in one run in the hope that they may assist crystal crushing (and hence dissolution) during stirring with a magnetic bar, and hence, accelerate deracemization. They had, though, no noticeable effect. Slow deracemization was observed, in a matter of weeks. At the beginning, composition stays nearly racemic in presence of thiourea amine for several days, before ee begins to rise gradually, indicating a prolonged lifetime of the metastable racemic non-equilibrium steady state.[28] Obviously, initiation time necessary for autocatalytic crystallization process to become effective is rather long under these conditions, resulting in delayed symmetry breaking. Once symmetry breaking starts, however, the system enters a dynamic state of constantly increasing ee, until eventually a new, ideally homochiral, and kinetically stable non-equilibrium steady state could be reached.[14]

Intriguingly, in all deracemization experiments, we recognized that a peak with retention time different from other known reaction components is growing at the expense of the peak pertaining to 1 in HPLC analysis of the reactions' crudes (Figure 11).

We were able to isolate a white precipitate that corresponds to that peak. By 1H-, 13C-NMR and mass analysis we were able to identify it as unsaturated hydrazone 12, product of condensation reaction between hydrazide 9 and ketone 10 (Figure 7 and Scheme 4), because it was also obtained as main product in aza-Michael reactions of 9 and 10 in presence of organic base in 70.3% (with 2) and 64.6% yield (with rac-3), respectively (Scheme 3b). Appearance of this condensation product at least demonstrates that reverse aza-Michael reaction step must have occurred in the reaction mixture, despite its high computed activation energy barrier.

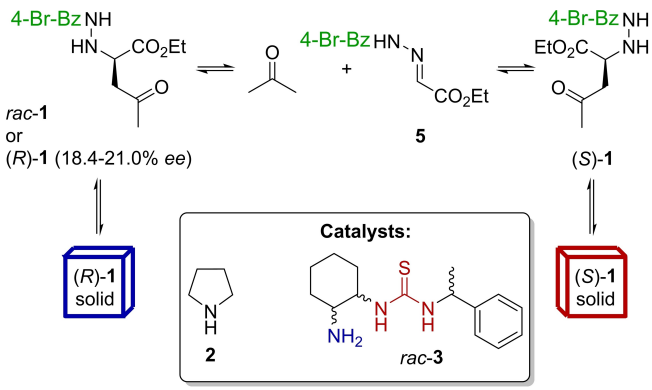

Scheme 5. Deracemization experiments with proposed racemization via forward and reverse steps,[16,17] starting from racemic or scalemic (18.4–21.0% *ee*) conglomerate mixtures of **1**.

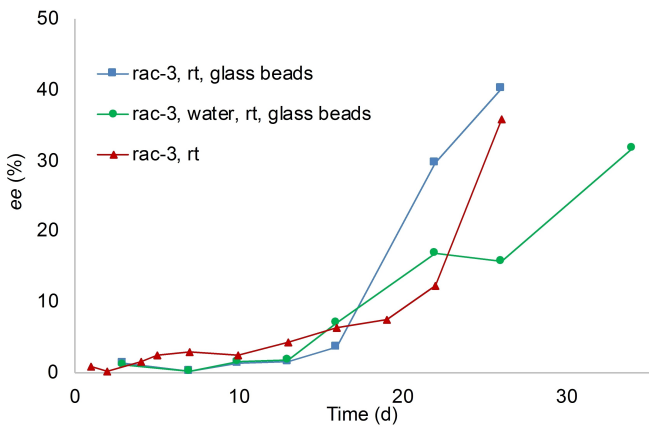

Figure 10. Deracemization experiments, starting from *rac*-**1** in presence of *rac*-**3** with (□) and without (△) added glass beads, and with H_2O as further additive (○).

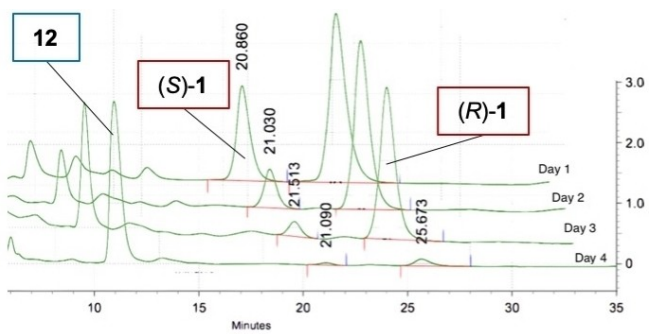

Figure 11. Comparison of HPLC chromatograms from samples taken every 24 hours during deracemization experiments in presence of *rac*-**3** performed at 40 °C and 1300 rpm on (*R*)-**1** with 20.4% initial *ee*.

This finding also explains not only the low mass balance (or retrieval rate) in 1, but also why we were always unable to reach a fully homochiral state in deracemization runs, because decomposition of 1 through side reactions dominates, when organic bases are allowed to act for several days on the reaction mixtures, especially at elevated temperatures (Figure 12).

In order to reduce observation time necessary in these experiments, we have henceforth used scalemic, rather than racemic, mixtures of 1 from the beginning of deracemization runs (Figures 12 and 13).

Surprisingly, we found high stirring rates to have an unexpected adverse effect on speed of deracemization (Figure 12). Apparently, acceleration of dissolution/crystallization process through high stirring rates may not be favorable, when racemization in solution phase is rate limiting, i.e. comparably slow. In further experiments, the higher stirring rate was kept nonetheless, in order to allow easy comparison of deracemization rate with that reported in other works and in which racemization was not rate limiting.[15]

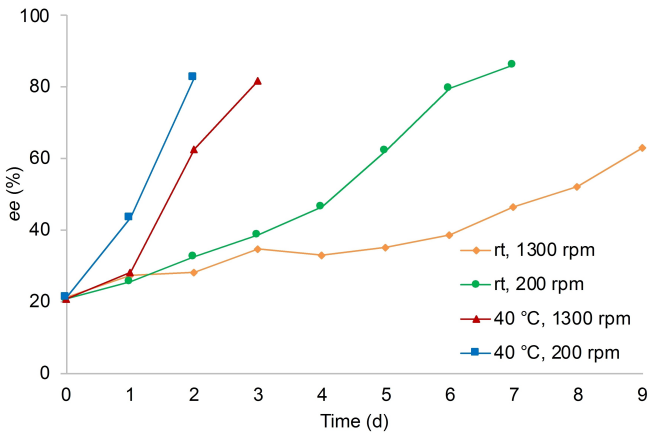

Figure 12. Deracemization experiments carried out on scalemic (*R*)-**1** (starting *ee* 21.0%) using *rac*-**3** (0.5 eq). Reaction conditions: a) room temperature and 1300 rpm (◇) or b) 200 rpm (○) stirring rate; or c) 40 °C and 1300 rpm (△) or d) 200 rpm (□) stirring rate.

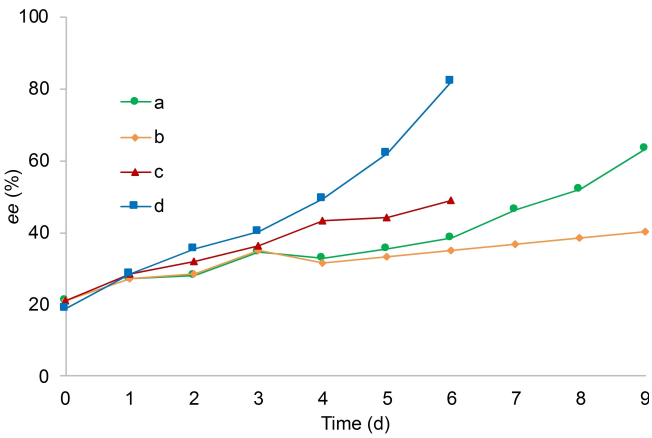

Figure 13. Deracemization experiments with *ee* values measured over ten days (*rac*-**3**) and six days (pyrrolidine **2**) in presence and in absence of H_2O, at rt and a stirring rate of 1300 rpm. Reaction conditions for runs **a**–**d** are reported in Table 2.

To our delight, addition of water and in presence of pyrrolidine as organic base results in significant (approximately 2-fold) increase in deracemization rate (Figure 13). Table 2 summarizes final ee values obtained after ten days (for rac-3) and after six days (for pyrrolidine), reflecting the fact that pyrrolidine was found to be the more active base in deracemization experiments. Following our computational predictions (Figure 8), water acts as co-catalyst to pyrrolidine in enolization, and because racemization is rate limiting when it is sufficiently slow, we experience an acceleration of deracemization. In presence of pyrrolidine and water (line d, Figure 13) we achieved 82.2% enantiomeric excess after six days, whereas we measured only 49.1% ee without water (line c) after the same time.

Curiously, and despite similarly observed acceleration of racemization by addition of water, when rac-3 is used as organic base, we found that behaviour of **2** and **3** in presence of water is opposite, with water acting as positive co-catalyst together with pyrrolidine, but as negative catalyst for the deracemization process in presence of thiourea amine, i.e. it slows it down. Except for higher concentration of 1 in deracemization experiments, as compared to that in racemization runs (Table 1), due to supersaturation, the only difference between racemizations in homogenous solution and our deracemization experiments is that the latter are carried out in a heterogenous system with a crystal-solution interface. Could water somehow interfere with the deracemization process, that is occurring at the crystal-solution interface? But if yes, why would it do so with thiourea, but not with pyrrolidine?

To explain this puzzling result, another riddle may come to our rescue: when Mannich and aza-Michael reactions are both viable but less favorable pathways for racemization, because of high barriers for their reverse steps, how is it possible that we could have earlier observed deracemization, requiring racemization, under water-free conditions at all?[16,17]

As we have earlier seen, enolization would prevail even under water-free conditions, but only when two pyrrolidine molecules co-act in the transition state. Much more likely would be to employ other organic bases, available in the reaction mixture, as enolization catalyst. Among them, hydrazine derivative 1 has certainly highest concentration in deracemization runs. Proton relay involved in energetically preferred stepwise enolization, assisted by two other molecules, requires a co-

Table 2. Reaction conditions in deracemization experiments with *rac*-**3** or pyrrolidine **2**, with and without added water as co-catalyst.

Entry[a]	ee_0 [%][b]	Cat [eq][c]	H_2O [eq][c]	ee_{high} [%][d]
a	21.0	*rac*-3 (0.5)	–	80.0
b	21.0	*rac*-3 (0.5)	1.0	42.9
c	21.0	2 (0.25)	–	49.1
d	18.9	2 (0.25)	1.0	82.2

[a] Entries in table correspond to lines in Figure 13. [b] Measured from pure scalemic **1** by chiral HPLC. [c] With respect to **1**. [d] Indicates highest final *ee* reached over evaluation time.

catalyst that functions as both proton acceptor and donor, like e.g. water, pyrrolidine, or indeed, like one of the N-basic sites in hydrazine derivative 1.

To our delight, we were able to locate computationally the enolization transition state structures with catalytic couple pyrrolidine-(R)-1 (Figure 14), and in which water (in Figure 8) or second pyrrolidine in a two-molecule mechanism is replaced by a molecule of chiral hydrazine derivative 1 itself, i.e. racemization proceeds through self-catalysis via a transition state structure for Cα deprotonation, only 0.7 kcal mol^{-1} higher in energy (with respect to the separated reactants) than T.S. 13 (Figure 8)! Unlike to the situation depicted in Figure 8, where pyrrolidine and water act as co-catalysts, transition state structure for C–O– protonation (corresponding to T.S. 14 in Figure 8, 0.2 kcal mol-1 lower in energy than T.S. 13) is 1.7 kcal mol^{-1} higher in energy than that for Cα deprotonation, and therefore rate limiting in autocatalytic enolization of 1. Corresponding encounter complex of (S)-1, (R)-1 and pyrrolidine is 3.2 kcalmol-1 less stable than that formed by (S)-1, pyrrolidine and water, probably due to strong hydrogen bridges, water is able to form.

Such an autocatalytic racemization is unusual,[29] and might be relevant also in racemization of amino acids, as they are also able to form enols.[30,31] Moreover, such spontaneous reactant-dependent autocatalysis appears to be yet unknown to organic chemists, even though an example was reported very recently for a (non-asymmetric) inorganic reaction and in which only reactant, rather than product, was catalyst in the spontaneous forward reaction step.[32]

Autocatalysis is commonly described as a process in which a reaction product catalyzes its own formation. Because product/catalyst needs to be produced first, before it can exert its catalytic activity, a sigmoidal reaction rate profile with an initiation phase is the consequence.[33] The reverse of an autocatalytic step is trivially reactant-catalyzed, of course. Hence, to avoid confusion, we limit the discussion here to spontaneous (i.e. exergonic) processes. Due to microreversibility, a catalyst must catalyze both forward and reverse reactions to the same extent. However, because of the second law of thermodynamics, only one direction (either forward or reverse) can be exergonic.[34] Here we propose therefore a spontaneous, entropy-driven type of autocatalysis, in which both reactant and product (which differs from reactant only in absolute configuration), can act as catalyst. Because reactant is available from the beginning of the reaction in sufficiently large amounts, an initiation phase or sigmoidal rate profile would not be observed in catalysis by reactant and which is not limited in scope to racemizations, i.e. narcissistic reactions.[32,34a] But only in such narcissistic reactions can both reactant and product be catalyst (and reaction velocity constant) – leaving aside the possibility of conceivable co-catalysis of physically different reactant and product molecules. Unlike self-accelerating catalysis by product,[35] catalysis by reactant alone is hence self-decelerating – unless reactant is present in excess.

Racemization being an asymmetric reaction, reaction rates, in principle, also depend on absolute configuration of reactant (or product) autocatalyst, similar to situation in asymmetric autocatalysis by chiral product molecules.[18] Hence, racemization rate could become dependent on concentration of enantiomers (and therefore on ee), and erosion of ee could

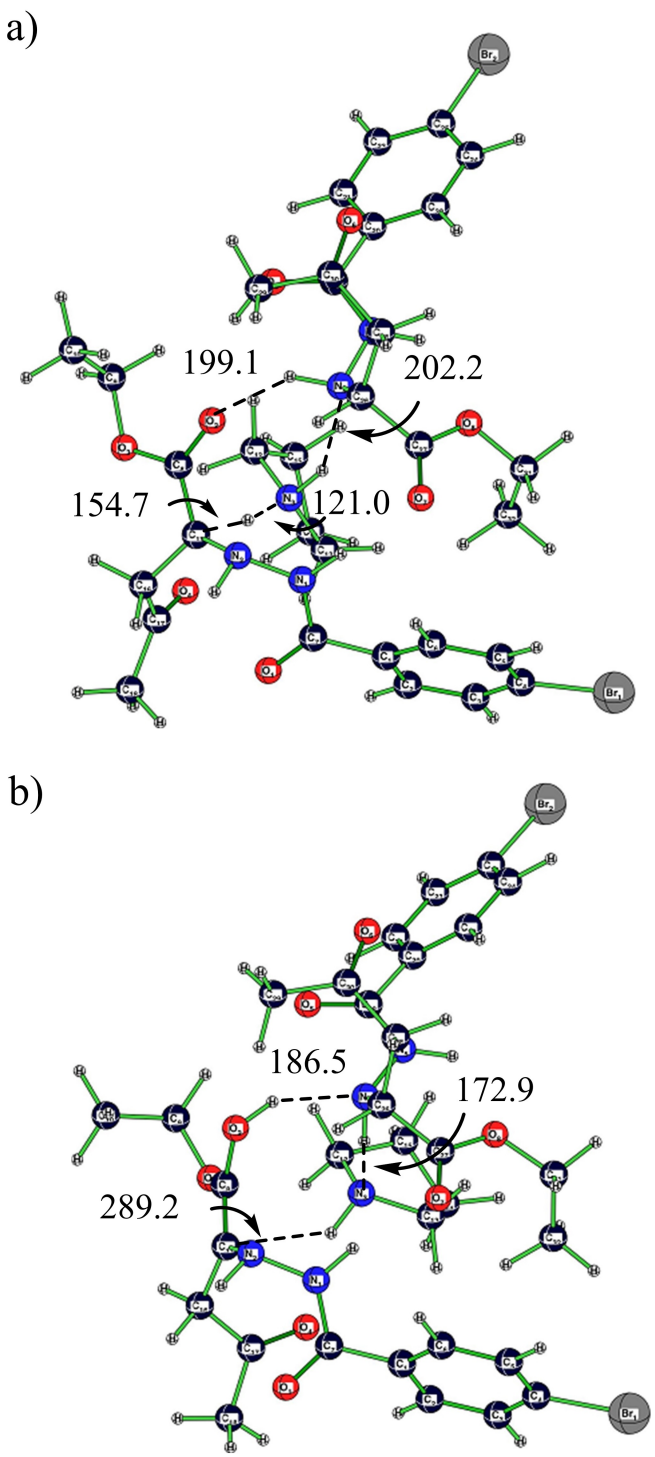

Figure 14. Computed M06-2X/6-31G* structures of a) C_α deprotonating and b) C-O$^-$ protonating transition states in reactant- (or product)-dependent heterochiral autocatalytic enolization of (*S*)-**1**, assisted by (*R*)-**1** and by pyrrolidine. Solvent effects have been included by polarizable continuum (PCM) model with electric permittivity of toluene. Selected bond lengths or distances are given in pm.

deviate from linearity in a direction, depending on whether a given enantiomer is transformed faster, when its racemization involves a catalyst of either same or of opposite enantiomer configuration, even though interplay of configuration and conformation is subtle.[35] Hence, apparent gradual acceleration of racemization under water-free conditions with thiourea (Figure 3, at 40 °C), could be an indication that heterochiral asymmetric autocatalysis might be somewhat favoured in homogenous solutions, while our findings under additional availability of a (*S*)-4 mimics' enantiopure crystal phase (Figure 4) remain inconclusive for heterogenous conditions in that respect.

Under water-free conditions, racemization hence is proposed to proceed predominantly autocatalytic, irrespective of organic base (pyrrolidine or thiourea amine 3) employed. This leaves open the possibility whether racemization occurs mostly deep in solution phase or at the crystal-solution interface. Water molecules can, of course, replace chiral hydrazine derivative 1 in the transition state structure (Figure 14). Depending on this competition between autocatalytic and water-catalyzed pathways for racemization via enolization, water could act in heterogenous systems presumably as a positive catalyst (together with pyrrolidine) or as a negative catalyst (together with thiourea amine), because, even though water catalysis may be less favorable than reactant autocatalysis, involving hydrazine derivative 1 as co-catalyst in presence of *rac*-3, water could block the background reaction, due to its unrivaled capability to form strong hydrogen bonds. This might also be an indication that the crystal-solution interface in a slurry could play a major role in both pyrrolidine and thiourea amine assisted racemization in absence of water, while in presence of water, solution phase racemization may dominate.

3. Conclusions

We have verified that intrinsically chiral compound **1** satisfies conditions for Viedma deracemization, namely that *rac*-**1** crystallizes as a conglomerate, and is able to racemize in solution phase in presence of an organic base. Furthermore, a detailed DFT study of available racemization pathways revealed, that aza-Michael/reverse aza-Michael and Mannich/reverse Mannich processes could contribute to some small extent, while distinctly preferred racemization pathway involves base-catalyzed enolization, both in presence of water and under water-free conditions.

Experimental evidence corroborated that reverse aza-Michael reaction steps do occur in the reaction mixture. Under water-free conditions, enolization is - based on computational findings - proposed to proceed via (asymmetric) autocatalysis and in which reactant and product (i.e. the enantiomers themselves) could both act as autocatalysts. Such autocatalytic racemization is unprecedented and self-catalysis by reactant, rather than product, could be a mostly overlooked possibility in many organic and inorganic reactions! Some experimental evidence has been also found for involvement of the conglomerates' crystal-solution interface in racemization.

Racemization is accelerated by presence of water, as we have computationally predicted and experimentally confirmed and in co-presence of both organic bases (pyrrolidine and *rac*-**3**). Viedma deracemization was experimentally shown to be sped up significantly by addition of water to the reaction mixture, when pyrrolidine was organic base employed. This is explained by water co-catalysis in enolization, as shown computationally, and confirms for the first time the rate limiting nature of racemization, instead of crystal growth,[15] for a Viedma deracemization process. In contrast, water slows down deracemization, when thiourea amine is base. These results can be rationalized by assuming a competition between water catalysis and reactant self-catalysis, which may lead to opposite results for the two organic bases.

The low fulfillment of the mass balance, found in our Viedma deracemization experiments, could be explained by yield reducing formation of an experimentally detected product generated through condensation reaction of a ketone and a hydrazide, produced in a reverse aza-Michael reaction step decomposing target compound **1** – a pathway that was also made plausible computationally.

When direct racemization of chiral product is an option, racemization via reverse reaction is unlikely to be favoured. On the other hand, and irrespective of actual mechanism of racemization, limitations by poorly performing (or even achiral) catalysts in enantioselective asymmetric synthesis, starting from achiral precursors, could be overcome by combination with Viedma ripening in analogy to asymmetric autocatalysis in homogenous systems.[17,35e,41] Analogously, application to diastereoselective asymmetric synthesis would also be possible, required that epimerization of individual chiral centers is selectively controlled,[42] extending the conglomerate concept to diastereomorphs or "quasi-enantiomorphs" (e.g. *R*–*S* and *R*–*R*), and when these neither differ too much in solubility nor their monomers' relative stability in a given solvent, in order to allow Viedma ripening. As the more stable diastereomer is likely to be the less soluble one, these could be conflicting goals, probably hard to reconcile in practice.

Methods Section

Computational Details

Geometry optimizations have been performed without any geometry restriction with GAUSSIAN09 program package.[36] We used a valence split 6-31G* Pople et al basis set[37] together with Zhao and Truhlar's M06-2X DFT functional,[38] which is re-parameterized to include dispersion energy effects. Solvent effects are simultaneously computed with Tomasi's and co-worker's polarized continuum (PCM) model,[39] assuming the electric permittivity of toluene. Stationary points have been rigorously characterized by harmonic frequency calculations. Cartesian coordinates of all computed species can be requested from the authors.

Experimental Details

All chemicals used for this work were purchased from commercial sources and were used without further purification. All solvents

were purified by distillation or were purchased in HPLC-grade-quality. Thin layer chromatography (TLC) was performed on pre-coated aluminium sheets ALUGRAM SIL G/UV254 (0,2 mm silica gel with fluorescent indicator, MachereyNagel & Co). Flash chromatography was performed with silica gel (Merck 60, particle size 0.040–0.063 mm). ^{1}H-NMR and ^{13}C-NMR were recorder at room temperature on Brucker Avance 300 and 400 spectrometers operating at 300 and 400 MHz. All chemical shifts are given in ppm-scale and refer to non-deuterized proportion of the solvent. The enantiomeric excess was determined by chiral HPLC analysis (with a chiral Chiralpak IA column) with comparison with authentic racemic material. HPLC measurements were performed with Agilent Technologies 1200 Series equipment.

Racemic ethyl 2-(2-(4-bromobenzoyl)hydrazineyl)-4-oxopentanoate (1): This compound was prepared as described in ref. [17], and it was isolated as a pale yellow solid in 31% yield. Spectroscopic data are in accordance with the literature. ^{1}H NMR (300 MHz, DMSO-d_6) δ 10.12 (d, J=6.5 Hz, 1 H), 7.79–7.61 (m, 4 H), 5.60 (t, J=6.1 Hz, 1 H), 4.04 (q, J=7.1 Hz, 2 H), 3.88 (dt, J=7.4, 5.6 Hz, 1 H), 2.88 (qd, J=17.6, 6.5 Hz, 2 H), 2.12 (s, 3 H), 1.12 (t, J=7.1 Hz, 3 H). ^{13}C NMR (101 MHz, DMSO) δ 205.9, 171.3, 164.8, 132.0, 131.4, 129.2, 125.2, 64.9, 62.0, 60.4, 58.1, 43.4, 30.1, 25.5, 15.2, 13.9. HRMS (ESI) calcd. for $C_{14}H_{18}BrN_2O_4$ $[M+H]^+$: 357.0444, found: 357.0432 $[M+H]^+$.

1-(2-aminocyclohexyl)-3-(1-phenylethyl)thiourea (3): This compound was prepared as described in ref. [17], and was isolated as a yellow solid, in 63% overall yield over two steps. Spectroscopic data are in accordance with the literature. ^{1}H NMR (400 MHz, DMSO-d_6) δ 7.41–7.08 (m, 5 H), 5.43 (s, 1 H), 3.38 (q, J=7.0 Hz, 1 H), 2.47–2.32 (m, 1 H), 1.95 (d, J=12.4 Hz, 1 H), 1.83–0.71 (m, 11 H). HRMS (ESI) calcd. for $C_{15}H_{24}N_3S$ $[M+H]^+$: 278.16855, found: 278.16851 $[M+H]^+$.

Ethyl 2-(2-(4-nitrobenzoyl)hydrazineyl)-4-oxopentanoate (4): This compound according to the synthetic procedure for **1**, described in ref. [16], and was isolated as a yellow solid, in 45% yield. ^{1}H NMR (400 MHz, DMSO-d_6) δ 10.37 (d, J=6.2 Hz, 1 H), 8.36–8.26 (m, 2 H), 8.05–7.97 (m, 2 H), 5.71 (t, J=6.1 Hz, 1 H), 4.05 (q, J=7.1 Hz, 2 H), 3.92 (dt, J=7.3, 5.7 Hz, 1 H), 3.01–2.81 (m, 2 H), 2.13 (s, 3 H), 1.13 (t, J=7.1 Hz, 3 H). ^{13}C NMR (101 MHz, DMSO-d_6) δ 205.8, 171.2, 163.9, 149.1, 138.5, 128.6, 123.6, 60.5, 58.0, 43.4, 30.0, 13.9. HRMS (ESI) calcd. for $C_{14}H_{17}N_3NaO_6$ [M+Na]: 346.1010, found: 346.1012 [M+Na].

Ethyl (*E*)-2-(2-(4-bromobenzoyl)hydrazineylidene)acetate (5): This compound was prepared as described in ref. [16], and was isolated as a white solid, in 70% yield. Spectroscopic data are in accordance with the literature. ^{1}H NMR (400 MHz, DMSO-d_6) δ 12.34 (s, 1 H), 7.97–7.63 (m, 5 H), 4.25 (q, J=7.1 Hz, 2 H), 1.27 (t, J=7.1 Hz, 3 H). ^{13}C NMR (101 MHz, DMSO-d_6) δ 164.6, 131.6, 130.0, 129.6, 60.9, 14.1. HRMS (ESI) calcd. for $C_{11}H_{12}BrN_2O_3$ $[M+H]^+$: 299.0026, found: 299.0033 $[M+H]^+$.

Ethyl (*E*)-4-oxopent-2-enoate (10): This compound was prepared as described in literature.[40] The product was isolated as a colourless oil, in 51% yield. Spectroscopic data are in accordance with the literature. ^{1}H NMR (400 MHz, DMSO-d_6) δ 6.92–6.67 (m, 2H), 4.21 (q, J=7.1 Hz, 2 H), 2.35 (s, 3 H), 1.25 (t, J=7.1 Hz, 3 H). ^{13}C NMR (101 MHz, DMSO) δ 199.1, 166.1, 141.0, 132.0, 61.9, 28.8, 14.8.

Ethyl (2*E*,4*E*)-4-(2-(4-bromobenzoyl)hydrazineylidene)pent-2-enoate (12): In two glass vials equipped with a stirring bar, the hydrazide **9** was dissolved in toluene. In each vessel the corresponding catalyst was added, namely Pyrrolidine (0.25 eq.) or *rac*-**3** (0.5 eq.), before Ethyl (*E*)-4-oxopent-2-enoate (**10**) was added. The reactions were allowed to stir at room temperature for 48 h. After this time, reactions were stopped, and the components separated and analyzed. Compound **12** was isolated by filtration directly from the reaction crude as a white solid, in 70% and 64% yield, using Pyrrolidine or *rac*-**3**, respectively. ^{1}H NMR (400 MHz, DMSO-d_6) δ 10.96 (s, 1 H), 7.99–7.56 (m, 4 H), 7.19 (s, 1 H), 6.41 (d, J=16.1 Hz, 1 H), 4.18 (q, J=7.1 Hz, 2 H), 2.15 (s, 3 H), 1.25 (t, J=7.1 Hz, 3 H). ^{13}C NMR (101 MHz, DMSO) δ 165.7, 144.3, 131.3, 60.4, 14.1, 12.4. HRMS (ESI) calcd. for $C_{14}H_{15}BrN_2O_3$ $[M+H]^+$: 339.0339, found: 339.0326 $[M+H]^+$.

General procedures for phase diagram studies: DSC measurements were performed on a DSC 131 (Setaram, France) at a heating rate of 2 K/min in temperature range from 25 to 160 °C using helium (5.0 purity) as purge gas. Samples of (*R*)-**1**, *rac*-**1** and differently composed mixtures of both were weighed into closed aluminium crucibles. Therefor calculated amounts of (*R*)-**1** and *rac*-**1** (altogether about 10 mg) were co-grounded in a mortar and dissolved in acetone. After solvent evaporation, the solid residue was crushed again and between 5 and 8 mg thereof used for DSC analysis. Determination of solidus and liquidus temperatures from the DSC curves was done as described in previous work.[19] Parallel to DSC, TG-DSC measurements (Sensys TG-DSC, Setaram, France) were used to study the thermal stability of selected samples ((*R*)-**1**, *rac*-**1**, 1:1 mixture thereof) in addition. Analysis conditions were similar to the DSC analyses: heating rate of 2 K/min in a temperature range of 25–170 °C, helium as purge gas and sample amounts between 8 and 12 mg.

XRPD measurements of (*R*)-**1** and *rac*-**1** were conducted on an X'Pert Pro diffractometer (PANalytical GmbH, Kassel, Germany) using Cu Kα radiation (λ=1.5418 Å) and an X'Celerator detector at ambient temperature. Samples of a few mg were prepared on zero background Si single crystal holders and scanned in a 2Θ range from 3 to 40° with a step size of 0.017° and a counting time of 100 s per step.

Hot Stage Microscopy (HSM) analyses were performed with an Axioscope 2 microscope (Carl Zeiss, Germany, magnification 20x/0.40) coupled with a temperature controlled hot stage (Linkam LTS420) and Axiovision imaging software. Few crystals of *rac*-**1** and (*R*)-**1** samples were dispersed on a glass microscope slide and placed on the hot stage sample holder. The physical changes and the complete melting of the crystals were observed over a temperature range of 25–150 °C with a heating rate of 2 K/min.

General procedure for racemization experiments: In homogeneous racemization experiments, compound **1** is completely dissolved in toluene in a vial equipped with a stirring bar. The solution is stirred for 5 minutes to homogenize before the opportune catalyst is added to the reaction mixture. In heterogeneous racemization experiments, compound *rac*-**4** is placed in a vial equipped with a stirring bar and toluene is added. The suspension is stirred for 5 minutes to homogenize and ensure that *rac*-**4** does not dissolve and that solid particles are present in the reaction mixture. Afterwards, compound **1** is added followed by the opportune catalyst. The experiments are stirred at rt or 40 °C during the evaluation time. Samples are taken from the reaction mixture every 24 h; in homogeneous racemization experiments 30 μL aliquots are placed in sample tubes, toluene is removed by means of a high vacuum pump (up to 10^{-3} mbar), and they are dissolved in HPLC grade isopropanol and analysed by chiral HPLC to determine the evolution of the *ee* during the time. In heterogeneous racemization experiments 30 μL aliquots are taken from reaction suspension and placed in an Eppendorf tube. By centrifuge (10000 rpm, 10 minutes) crystal and solution phases are separated, toluene is evaporated by means of a high vacuum pump (up to 10^{-3} mbar), then both samples are dissolved in HPLC grade isopropanol and independently analysed by chiral HPLC to determine racemization rates.

General procedure for deracemization experiments: Racemic or scalemic (~20% *ee*) **1** is placed in a vial equipped with a stirring bar (in selected experiments glass beads were also present) and the opportune amount of toluene (0.224 mM) is added. The suspension is stirred for 5 minutes to homogenize and ensure that compound **1** does not completely dissolve; then the opportune catalyst is added to the suspension. The reaction mixture is stirred at rt or 40 °C during the evaluation time. Samples are taken from the reaction mixture every 24 h. 30 μL aliquots are taken from the reaction suspension and placed in an Eppendorf tube. By centrifuge (10000 rpm, 10 minutes) crystal and solution phases are separated, toluene is evaporated by means of a high vacuum pump (up to 10^{-3} mbar), then they are dissolved in HPLC grade isopropanol and independently analysed by chiral HPLC to determine racemization rates.

Acknowledgements

*This research received funding as part of the CORE ITN Project by the European Union Horizon 2020 Research and Innovation Program under the Marie Skłodowska-Curie Grant Agreement No. 722456 CORE ITN. We also thank the Interdisciplinary Center for Molecular Materials (ICMM), the Graduate School Molecular Science (*GSMS*) for research support*. Open access funding enabled and organized by Projekt DEAL.

Conflict of Interest

The authors declare no conflict of interest.

Keywords: autocatalysis · deracemization · enolization · racemization · stereochemistry

[1] a) A. Calcaterra, I. D'Acquarica, *J. Pharm. Biomed. Anal.* **2018**, *147*, 323; b) I. Agranat, H. Caner, J. Caldwell, *Nat. Rev. Drug Discovery* **2002**, *1*, 753.
[2] I. Agranat, H. Caner, *Drug Discov. Today* **1999**, *4*, 313.
[3] A. Mullard, *Nat. Rev. Drug Discov.* **2012**, *11*, 91.
[4] I. Agranat, S. R. Wainschtein, *Drug Discov. Today* **2010**, *15*, 163.
[5] I. Agranat, S. R. Wainschtein, E. Z. Zusman, *Nat. Rev. Drug Discov.* **2012**, *11*, 972.
[6] E. J. Ariëns, *Eur. J. Clin. Pharmacol.* **1984**, *26*, 663.
[7] a) R. A. Sheldon, *Drug Inf. J.* **1990**, *24*, 129; b) D. L. Hughes, *Comprehensive Chirality*, Elsevier, Amsterdam, **2012**, pp. 1–26.
[8] a) L. A. Nguyen, H. He, C. Pham-Huy, *Int. J. Biomed. Sci.* **2006**, *2*, 85; b) H. Leek, L. Thunberg, A. C. Jonson, K. Öhlén, M. Klarqvist, *Drug Discov. Today* **2017**, *22*, 133; c) R. Siedlecka, *Tetrahedron* **2013**, *69*, 6331.
[9] E. Fogassy, M. Nogradi, D. Kozma, G. Egri, E. Palovics, V. Kiss, *Org. Biomol. Chem.* **2006**, *4*, 3011.
[10] a) E. Sanganyado, Z. Lu, Q. Fu, D. Schlenk, J. Gan, *Water Res.* **2017**, *124*, 527; b) I. Ilisz, A. Aranyi, Z. Pataj, A. Péter, *J. Chromatography A* **2012**, *1269*, 94; c) R. W. H. Perera, I. Abraham, S. Gupta, P. Kowalska, D. Lightsey, C. Marathaki, N. S. Singh, W. J. Lough, *J. Chromatography A* **2012**, *1269*, 189; d) A. R. Ribeiro, A. S. Maia, Q. B. Cass, M. E. Tiritan, *J. Chromatography B* **2014**, *968*, 8.
[11] A. H. Kamaruddin, M. H. Uzir, H. Y. Aboul-Enein, H. N. A. Halim, *Chirality* **2009**, *21*, 449–467.
[12] J. Dalmolen, T. D. Tiemersma-Wegman, J. W. Nieuwenhuijzen, M. van der Sluis, E. van Echten, T. R. Vries, B. Kaptein, Q. B. Broxterman, R. M. Kellogg, *Chem. Eur. J.* **2005**, *11*, 5619.
[13] a) C. Viedma, *Phys. Rev. Lett.* **2005**, *94*, 065504; Already earlier, spontaneous deracemization on stirring slurries of intrinsically chiral compounds under their saturated solutions was found, but overlooked for decades, see: b) E. Havinga, *Biochem. Biophys. Acta* **1954**, *13*, 171; Even before publication of the mss. ref. 13a, Uwaha explained the results based on a nonlinear autocatalytic crystal growth mechanism involving cluster formation, see: c) M. Uwaha, *J. Phys. Soc. Jpn.* **2004**, *73*, 2601.
[14] a) W. L. Noorduin, W. J. P. V. Enckevort, H. Meekes, B. Kaptein, R. M. Kellogg, J. C. Tully, J. M. McBride, E. Vlieg, *Angew. Chem. Int. Ed.* **2010**, *49*, 8435; Due to autocatalytic nature of crystal growth, conglomerate deracemization can be also achieved through exploitation of thermal hysteresis (i.e. cycles of cooling and heating), see, e.g.: b) W. W. Li, L. Spix, S. C. A. de Reus, H. Meekes, H. J. M. Kramer, E. Vlieg, J. H. ter Horst, *Cryst. Growth Des.* **2016**, *16*, 5563.
[15] W. L. Noorduin, T. Izumi, A. Millemaggi, M. Leeman, H. Meekes, W. J. P. Van Enckevort, R. M. Kellogg, B. Kaptein, E. Vlieg, D. G. Blackmond, *J. Am. Chem. Soc.* **2008**, *130*, 1158.
[16] S. B. Tsogoeva, S. Wei, M. Freund, M. Mauksch, *Angew. Chem. Int. Ed.* **2009**, *48*, 590.
[17] S. Wei, M. Mauksch, S. B. Tsogoeva, *Chem. Eur. J.* **2009**, *15*, 10255.
[18] M. Mauksch, S. B. Tsogoeva, I. M. Martynova, S. Wei, *Angew. Chem. Int. Ed.* **2007**, *46*, 393.
[19] H. Lorenz, *Crystallization - Basic Concepts and Industrial Applications* (Ed.: W. Beckmann), Wiley-VCH, Weinheim, **2013**, pp. 35–74.
[20] Viedma, Kellogg, Blackmond and co-workers had already established, that physically, presence of an enantiopure solid phase has no influence on racemization rate and that rates in presence of such a phase in heterogenous systems appear lower by a factor of two than they actually are, because depleted enantiomer is replenished from solid phase. However, we have used here mimics of racemizing compound to separate racemization from this replenishment. In contrast, we state that solid-solution interface may be chemically, rather than physically, involved in the racemization process; C. Viedma, C. J. V. Verkuijl, J. E. Ortiz, T. de Torres, R. M. Kellogg, D. G. Blackmond, *Chem. Eur. J.* **2010**, *16*, 4932.
[21] Solubility of quasi-enantiomeric nitro compound **4** is somewhat higher than that of **1**, so that is added in amounts large enough to compensate for the dissolved part.
[22] a) R. R. E. Steendam, J. M. M. Verkade, T. J. B. Van Benthem, H. Meekes, W. J. P. Van Enckevort, J. Raap, F. P. J. T. Rutjes, E. Vlieg, *Nat. Commun.* **2014**, *5*, 5543; Because aza-Michael product generated in this reaction is non-enolizable, in contrast to **1**, its likely deprotonation by DBU yields actually a rapidly inverting "flat" (154° dihedral angle at stereocenter) carbanion via a conformationally chiral transition state structure involved in preferred racemization mechanism, with an activation barrier of only 3.8 $kcalmol^{-1}$ (at M06-2X/6-31G* level). This carbanion inversion connects two non-superimposable enantiomeric conformations, which are rotamers from internal rotation of the acetyl group. Optically stable carbanions are very rare, see for an example:b) M. M. Olmstead, P. P. Power, *J. Am. Chem. Soc.* **1985**, *107*, 2174.
[23] C. E. Yeom, M. J. Kim, B. M. Kim, *Tetrahedron* **2007**, *63*, 904.
[24] H. M. Niemeyer, *Tetrahedron* **1977**, *17*, 2267.
[25] Z. Yao, B. Dai, Y. Yu, H. Ji, L. Zhou, K. Cao, *RSC Adv.* **2017**, *7*, 10881.
[26] We assume here that enolate is protonated swiftly (probably in a barrierless process, therefore at kinetic diffusion limit) and preferably at oxygen, rather than at C_α carbon, and involving a proton different from that initially removed from C_α (two-proton mechanism). Uncatalyzed keto-enol tautomerization has a high energy barrier. Tertiary amines like DBU only support step-wise or concerted one-proton mechanisms. Acid catalyzed enolization is also possible, of course, involving initial protonation at carbonyl oxygen and therefore polarization of the C=O bond. Acid and base catalysis can occur simultaneously but non-synchronously, e.g. in active centers of enzymes. Water-catalyzed enolization is already known, see e.g: G. Alagona, C. E. Ghio, P. I. Nagy, *Phys. Chem. Chem. Phys.* **2010**, *12*, 10173; In principle, proton relay in enolization may be concerted, irrespective of molecularity (i.e. number of catalyst molecules involved in transition state structure). We have found here, however, only tautomerization with step-wise proton relay (X = N or O and moving proton marked bold-face, while other protons take part in hydrogen-bridging): with two catalytic molecules, C···**H(1)**···X(1)···H(2)···X(2)···H(3)···O in the first step and C···H(1)···X(1)···**H(2)**···X(2)···**H(3)**···O in second step, or, with a single catalytic molecule, C···**H(1)**···X···H(2)···O in the first and C···H(1)···X···**H(2)**···O in second step. Combinatorically, with four different basic species (water, pyrrolidine, thiourea amine **3**, hydrazine derivative **1**) and two molecules involved in transition state structure, there are 144 different transformation pathways possible (note that **1** and **3** are chiral, and additionally,

contain more than one chemically distinct basic site), of which we have studied only four here.
[27] T. Kawabata, S. Kawakami, S. Majumdar, *J. Am. Chem. Soc.* **2003**, *125*, 13012.
[28] C. Blanco, J. Crusats, Z. El-Hachemi, A. Moyano, S. Veintemillas-Verdaguer, D. Hochberg, J. Ribó, *ChemPhysChem* **2013**, *14*, 3982.
[29] However, see for a decades old proposal of base-catalyzed and partly autocatalytic racemization of oxazolones: M. Slebioda, M. A. St. Amand, F. M. F. Chen, N. L. Benoiton, *Can. J. Chem.* **1988**, *66*, 2540; See SI for a more detailed conceptual development of autocatalytic enantiomerization and racemization.
[30] Note that compound **1** could be considered an amino acid derivative. Amino acids had indeed been found to racemize via (reversible) first order kinetics, see e.g. J. L. Bada, *J. Am. Chem. Soc.* **1972**, *94*, 1371.
[31] Even though two molecules of racemizing compound are involved in transition state structure (see e.g. Figure 14), racemization might still follow a first order kinetics when rates for processes catalyzed by same and opposite enantiomers do not differ, because total concentration of enantiomers is, of course, constant.
[32] Reactant-dependent autocatalysis has been reported for reaction of SO_3 and NH_3 to give sulfamic acid, catalyzed by ammonia, see: H. Li, J. Zhong, H. Vehkamäki, T. Kurtén, W. Wang, M. Ge, S. Zhang, Z. Li, X. Zhang, J. S. Francisco, *J. Am. Chem. Soc.* **2018**, *140*, 11020.
[33] T. Sawato, N. Saito, M. Yamaguchi, *ACS Omega* **2019**, *4*, 5879.
[34] Racemization described here comprises of automerization (*R*-to-*R*, *S*-to-*S*) and enantiomerization (*R*-to-*S* and vice versa) steps, i.e. narcissistic reactions, see: a) L. Salem, *Acc. Chem. Res.* **1971**, *4*, 322; While automerization occurs as a dynamic equilibrium process, enantiomerization is driven at non-equilibrium by approaching maximum entropy for racemic composition, see: b) D. Kondepudi, I. Prigogine, *Modern Thermodynamics*, 2nd ed., John Wiley & Sons Inc., New York, **2009**.
[35] Classical product-dependent autocatalysis is considered to require that autocatalytic step is rate limiting, exergonic, and catalysis positive. Moreover, if several competing elementary reaction steps (i.e. on different pathways) exist, autocatalytic steps need to be the fastest to be recognizable. In this case, a sigmoidal rate profile, rate acceleration, thermal hysteresis and seeding effects could be observed, for a review see e.g.: a) A. J. Bissette, S. P. Fletcher, *Angew. Chem. Int. Ed.* **2013**, *52*, 12800; In contrast, asymmetric autocatalysis, i.e. processes of type $A+R \rightarrow 2\ R$ (homochiral) and $A+R \rightarrow R+S$ (heterochiral) with a prochiral reactant A, involve transfer of chirality information from chiral product (i.e. *R* or *S*) to A, and is not necessarily rate accelerating or resulting in chiral amplification (see e.g. ref. 18). Asymmetric autocatalysis with chiral amplification is possible only with homochiral type through additional either hypercompetitive, e.g. $A+2\ R \rightarrow 3\ R$, or mutually inhibiting reaction steps $R+S \rightarrow$ P (or 2 P), with an inactive product P, see: b) P. Decker, *J. Mol. Evol.* **1973**, *2*, 137; c) K. Iwamoto, M. Seno, *J. Chem. Phys.* **1982**, *76*, 2347; d) F. C. Frank, *Biochim. Biophys. Acta* **1953**, *11*, 459; For an experimental realization of hypercompetitive type, see: e) K. Soai, T. Shibata, H. Morioka, K. Choji, *Nature* **1995**, *378*, 767.
[36] GAUSSIAN09, M. J. Frisch, et al., Gaussian Inc. Pittsburgh PA, **2008**.
[37] R. Krishnan, J. S. Binkley, R. Seeger, J. A. Pople, *J. Chem. Phys.* **1980**, *72*, 650.
[38] Y. Zhao, D. G. Truhlar, *Theor. Chem. Acc.* **2008**, *120*, 215.
[39] J. Tomasi, B. Mennucci, R. Cammi, *Chem. Rev.* **2005**, *105*, 2999.
[40] J. E. Taylor, A. T. Davies, J. J. Douglas, G. Churchill, A. D. Smith, *Tetrahedron: Asymmetry* **2017**, *28*, 355–366.
[41] See for symmetry breaking in a system blurring barrier between homogenous and heterogenous systems: T. Reppe, S. Poppe, X. Cai, Y. Cao, F. Liu, C. Tschierske, *Chem. Sci.* **2020**, *11*, 5902.
[42] See for application of Viedma ripening to a diastereomeric compound, involving a conglomerate of *R*-*R* and *S*-*S* enantiomorphs: A. H. J. Engwerda, J. C. J. Mertens, P. Tinnemans, H. Meekes, F. P. J. T. Rutjes, E. Vlieg, *Angew. Chem. Int. Ed.* **2018**, *57*, 15441.

Manuscript received: July 13, 2020
Accepted manuscript online: June 9, 2020
Version of record online: ■■, ■■■